A novel method to measure calcium carbonate with portable X-ray fluorescence instrumentation and its application to Gulf of Mexico surficial sediments

Article *in* Sedimentary Geology · July 2020

DOI: 10.1016/j.sedgeo.2020.105724

CITATIONS
5

READS
168

6 authors, including:

Miguel Angel Huerta-Diaz
Autonomous University of Baja California (Universidad Autónoma de Baja Califor…
93 PUBLICATIONS **3,469** CITATIONS
SEE PROFILE

Jacob Alberto Valdivieso-Ojeda
Autonomous University of Baja California
15 PUBLICATIONS **87** CITATIONS
SEE PROFILE

Francisco Delgadillo-Hinojosa
Autonomous University of Baja California
63 PUBLICATIONS **965** CITATIONS
SEE PROFILE

Karla Mejia
Autonomous University of Baja California
8 PUBLICATIONS **59** CITATIONS
SEE PROFILE

Sedimentary Geology 406 (2020) 105724

Contents lists available at ScienceDirect

Sedimentary Geology

journal homepage: www.elsevier.com/locate/sedgeo

A novel method to measure calcium carbonate with portable X-ray fluorescence instrumentation and its application to Gulf of Mexico surficial sediments

Jonathan Garcia-Orozco [a], Miguel Angel Huerta-Diaz [b,*], Jacob Alberto Valdivieso-Ojeda [b], Francisco Delgadillo-Hinojosa [b], Karla Gabriela Mejia-Piña [c], Flor Árcega-Cabrera [d]

[a] Posgrado en Oceanografía Costera, Instituto de Investigaciones Oceanológicas/Facultad de Ciencias Marinas, Universidad Autónoma de Baja California (UABC), Apdo. Postal 76, Ensenada, Baja California 22800, Mexico
[b] Instituto de Investigaciones Oceanológicas, UABC, Apdo. Postal 453, Ensenada, Baja California 22800, Mexico
[c] Facultad de Ciencias Marinas, UABC, Apdo. Postal 76, Ensenada, Baja California 22800, Mexico
[d] Unidad de Química Sisal, Facultad de Química, Universidad Nacional Autónoma de México, Puerto de Abrigo S/N, Sisal, Yucatán, 97355, Mexico

ARTICLE INFO

Article history:
Received 14 May 2020
Received in revised form 3 July 2020
Accepted 4 July 2020
Available online 11 July 2020

Editor: Dr. Jasper Knight

Keywords:
XRF
Authigenic calcium
Inorganic carbon
Organic carbon
Titanium

ABSTRACT

A novel, rapid, low cost, non-destructive and reliable technique was developed to simultaneously measure calcium carbonate ($CaCO_3$) and trace element concentrations in sediments with a portable X-ray fluorescence (pXRF) analyzer, and applied to 27 samples of surficial sediments collected from the Yucatán continental shelf (<230 m water depth) and 33 samples from deep sediments (>1200 m water depth) of the Gulf of Mexico. This technique is based on calculation of authigenic calcium (Ca_{auth}) from the total Ca measured with the pXRF. Results obtained with the pXRF showed a very high and highly significant correlation ($r = 0.99$, $P < 0.001$) with measurements of inorganic carbon (C_i) obtained by coulometry, with a slope of 0.972 ± 0.014 SD and negative Y-intercept of -0.403 ± 0.093 SD. The latter is consistent with the presence of carbonates unrelated to Ca (e.g., $MgCO_3$, $SrCO_3$, $MnCO_3$, $FeCO_3$) that were not detected by the pXRF. Statistical analysis indicated that the means of C_i and Ca_{auth} did not differ significantly, thus yielding reliable measurements with the pXRF. The C_i concentrations can be calculated directly from Ca_{auth} or, alternatively, from several sediment samples measured by coulometry (or other reliable method) whereby C_i can be calculated from the linear regression between these two parameters. Finally, Ca_{auth} and titanium showed an inverse relationship, suggesting that carbonates act as diluents of terrigenous material, especially in the western side of the Gulf of Mexico where riverine transport of this land-derived material is more intense.

1. Introduction

Carbonate sediments reflect climatic changes throughout the Earth's history (Falkowski et al., 2000), given that a large portion of global carbon is found stored in this type of sediments (Roberts et al., 2013). For example, it has been calculated that ~20% of sedimentary rocks from the Phanerozoic are composed of carbonate minerals (Morse and Arvidson, 2002). In the last three decades, interest in the study of carbonates in the marine environment has increased due to the impact of carbon dioxide (CO_2), generated by fossil fuel combustion (e.g., Ridgwell and Zeebe, 2005; Lenton and Britton, 2006). The production of calcium carbonate can exacerbate climate change and even accelerate ocean acidification, whereas its dissolution can serve as a CO_2 sink (e.g., Broecker and Peng, 1987; Opdyke and Walker, 1992; Archer and Maier-Reimer, 1994; Macreadie et al., 2017). Additionally, current estimates of so-called blue carbon, defined as the carbon sequestered in vegetated coastal ecosystems (Mcleod et al., 2011), are primarily focused on organic carbon, while overlooking the role played by calcium carbonate ($CaCO_3$) in the carbon cycle (e.g., Macreadie et al., 2017; Saderne et al., 2019; Sanders et al., 2019). From an economic standpoint, it has been calculated that ~50% of the global volume of hydrocarbon reserves is found in carbonate sediments, which can also contain ore deposits (Blatt et al., 1980).

It has been calculated that ~25×10^{12} moles y^{-1} of carbonates are produced in the upper 100 m of the current ocean, out of which 15×10^{12} moles y^{-1} end up accumulating in shallow sediments (Schneider et al., 2000). By contrast, in deep sediments, representing an area of 320×10^6 km^2, ~68.5×10^{12} moles y^{-1} of carbonates are produced in overlying waters, out of which ~17×10^{12} mol y^{-1} end up accumulating in sediments (Schneider et al., 2000). The difference between shallow and deep sediments is due to the fact that they differ in their carbon

* Corresponding author.
E-mail address: huertam@uabc.edu.mx (M.A. Huerta-Diaz).

https://doi.org/10.1016/j.sedgeo.2020.105724
0037-0738/

sources, specific mineralogy, accumulation processes (Morse and Mackenzie, 1990) and dissolution below the carbonate compensation depth (Ben-Yaakov et al., 1974). For example, shallow sediments are generally dominated by aragonite and calcite rich in magnesium (Mg), produced by the disintegration of skeletons of benthic organisms (Morse and Mackenzie, 1990; Schneider et al., 2000). In contrast, deep sea sediments rich in carbonates are composed of calcite low in Mg (>99% $CaCO_3$) derived from remains of coccolithophorids and pelagic foraminifera (Morse and Mackenzie, 1990; Roberts et al., 2013).

Different methodologies are used to measure the concentration of inorganic carbon (essentially $CaCO_3$), some of which are labor-intensive, and characterized by varying degrees of precision and accuracy. Among the more commonly used techniques is the loss on ignition method (LOI) (Dean, 1974; Wang et al., 2012b), involving the conversion of carbon to CO_2 via sequential heating of the sample to 550 °C (organic carbon) and 950 °C (inorganic carbon). The difference in weight obtained in each of the two steps is proportional to the organic (C_{org}) and inorganic (C_i) carbon of the sample, respectively (Heiri et al., 2001; Santisteban et al., 2004). However, LOI has the disadvantage that these relationships are affected by the composition of the sediment (e.g., Santisteban et al., 2004). Another method, referred to as the Scheibler method, involves treating the samples with HCl and measuring the released CO_2 volumetrically (Tatzber et al., 2007), which can yield high-quality C_i results (Wang et al., 2012a). Instrumentation for the analysis of carbon, like automatic CHNS analyzers, can measure C_{org} and C_i directly, and is also capable of determining total concentrations of nitrogen and sulfur (e.g., Kristensen and Andersen, 1987; Ryba and Burgess, 2002; Andrade et al., 2009; Rabouille et al., 2009). The underlying principle of these instruments is the catalytic combustion of the sample at high temperatures to produce N_2, SO_2 and CO_2, which are measured with an infrared detector (e.g., Wang et al., 2012a). Finally, coulometric determination of C_{org} and C_i concentrations is available, involving the acidification and/or combustion of the sample to generate CO_2, which is measured quantitatively in an electrochemical cell (Huffman, 1977; Engleman et al., 1985; Johnson et al., 1985, 1987).

The main disadvantage of all the measurement techniques mentioned above is that they destroy the sample (which in most cases yield only the C_i concentration), involve high maintenance and operation costs, and some are labor-intensive, time-consuming and/or inaccurate. In this study, a non-destructive analytical technique is developed that uses a portable X-ray fluorescence instrument (pXRF), with which it is possible to estimate $CaCO_3$ concentrations and simultaneously measure the total concentrations of up to 27 elements (e.g., Mejía-Piña et al., 2016). Mineral assessment using a pXRF has been previously reported by Kessler and Nagarajan (2012), who indirectly estimated clay contents in sedimentary rocks using Rb as a proxy. Additionally, well established analytical techniques have been developed based on pXRF instruments, including applications in meteorite research (Crupi et al., 2014), geochemical exploration (Arne et al., 2014; Yuan et al., 2014), contamination studies (Vanhoof et al., 2004; Parsons et al., 2013; Lemiere et al., 2014), and chemostratigraphy and geochemistry (Rowe et al., 2012; Dahl et al., 2013; Ibañez-Insa et al., 2017; Sinnesael et al., 2018; Hines et al., 2019; Saker-Clark et al., 2019). Furthermore, methodologies to specifically study the geochemistry of carbonates (e.g., mollusk shells, fossils, sediments, corals, bones, eggs, speleothems) in the laboratory and in situ have been developed by a number of researchers using pXRF (Rodríguez-Navarro et al., 2008; Moreno et al., 2013; Quye-Sawyer et al., 2015; Anbu et al., 2016; D'Elia et al., 2016; de Winter and Claeys, 2017; de Winter et al., 2017; Sinnesael et al., 2018; Arenas-Islas et al., 2019).

The advantages of our method include: (a) it does not destroy the sample, preserving its integrity for other types of analyses, (b) samples do not require additional or special treatment, (c) results for each sample are obtained in ~6 min, (d) operational costs are low, and finally (e) in situ measurements in the field are feasible once the instrument is calibrated (however, see Potts et al., 1997, 2006 and Quye-Sawyer et al., 2015 for inhomogeneities and surface effects). Results of $CaCO_3$ concentrations inferred from pXRF analysis of Ca and Al measured in 60 surficial marine sediment samples are here compared with measurements conducted by coulometry: 33 samples are distributed along the deep portion of the Gulf of Mexico (>1200 m) and 27 samples were collected in the shallow (<230 m) Yucatán continental shelf, Mexico. Results of this analysis show that our novel method provides a low cost, rapid and reliable means of measuring $CaCO_3$ present in marine sediments.

2. Description of the study area

The Gulf of Mexico is found at mid- and low-latitudes, occupying an area of ~1.5×10^6 km^2 (Balsam and Beeson, 2003). A fraction of its sediment constituents are generated by geochemical or biogenic processes; however, most sediments are supplied by river transport from the large terrestrial masses adjacent to the Gulf (Davis, 2017; Ward and Tunnell Jr., 2017). The pelagic sedimentary environment of the Gulf of Mexico is similar to those of other global oceans with relatively flat surfaces and local relief of a few meters (Davis, 2017). Its sediments tend to be dominated by sludge made up of fine-grained terrigenous material composed of aluminosilicate material (clays) and biogenic sediments (Davis, 2017; Ward and Tunnell Jr., 2017). In the abyssal plains of the Gulf of Mexico, the main input of terrigenous sediment is via gravitational processes, such as turbidity currents, and to a lesser degree, by water column settlement (Davis, 2017). Mean clay (<2 μm) and silt (2–63 μm) fractions of the sediments range between 18%–30% and 59%–74%, respectively, with most displaying more than 90% silt + clay content (Diaz-Asencio et al., 2019). Generally, there is a balance between terrigenous and carbonate components in the deep sediments of the Gulf of Mexico, with the former ranging between 26 and 81 dw% (Diaz-Asencio et al., 2019).

The concentrations of $CaCO_3$ in Gulf of Mexico sediments lie in the range of 0% to >90% and generally increase from northwest to southeast (Davies and Moore, 1970; Balsam and Beeson, 2003). Carbonates in deep waters of the Gulf of Mexico tend to be preserved because they are saturated with respect to carbonate (Diaz-Asencio et al., 2019). However, sediments with the highest $CaCO_3$ concentrations (>75%; Balsam and Beeson, 2003) are found in the two main carbonate provinces of the Gulf, the Yucatán and Florida continental shelves, where carbonates are mostly of biogenic origin (Ward and Tunnell Jr., 2017). The Yucatan continental shelf is a smooth, broad platform with carbonate sediments of variable texture and complex seabed topography (Logan et al., 1969; Balsam and Beeson, 2003) and a reduced slope with low depths (maximum of 200 m). At its northern margin is located the Campeche Escarpment and to the east the Caribbean Sea. The Yucatan platform is a submerged northeastward extension (~300 km) of the Yucatan continental shelf, formed by a limestone and calcium carbonate block (Logan et al., 1969). Sediments of the Yucatan Peninsula are mainly composed of carbonates from the Pleistocene and Holocene (Aguayo et al., 1980), with ages of between 20,000 to 30,000 years (Ward and Wilson, 1976). On the Yucatán shelf it is also possible to find carbonate muds, although sediments are mainly composed of carbonate sand derived from reefs that include ooids, fragments of skeletons (mollusks, foraminifera, algae, echinoids, corals and bryozoans), pellets and carbonate clasts (Davies and Moore, 1970; Balsam and Beeson, 2003; Davis, 2017; Ward and Tunnell Jr., 2017).

The C_{org} concentrations of terrigenous origin preserved in Gulf of Mexico sediments are relatively high (<10% of total organic material) due to the fact that the Gulf system is almost completely surrounded by the continental mainland (Hedges and Parker, 1976; Goñi et al., 1997). However, an important input of organic matter occurs as a discharge of natural petroleum, which is widely distributed in the Gulf. In particular, deep Gulf of Mexico sediments represent one of the most prolific worldwide zones of natural discharges of hydrocarbons and gas (Ward and Tunnell Jr., 2017).

3. Materials and methods

The 33 surficial samples of the deep Gulf of Mexico sea floor used in this study were collected on board the *R/V Justo Sierra*, during five oceanographic cruises (XIXIMI-1 to XIXIMI-5) carried out between November 2010 and June 2016. All the sediment samples were collected at depths of 1242 to 3801 m (Table S1, Fig. 1) using multiple or box type corers. Immediately following collection, the sediment cores were sectioned at 1 or 2 cm intervals with a plastic spatula to avoid metal contamination. Each sediment section was stored in a labeled Ziploc® plastic bag and refrigerated at −4 °C until analysis in the laboratory. For the purpose of this study, only samples closest to the water-sediment interface of each core were used to infer $CaCO_3$ concentrations (Table S1). Additionally, 27 samples of surficial sediments (<230 m water depth) were collected with a Smith-McIntyre® dredge on the shelf and slope of the Yucatán Peninsula, during oceanographic cruises GOMEX-04 and GOMEX-05 (November 2015 and September 2016, respectively), carried out on board the *R/V Riviera Maya* (Table S2, Fig. 1). Once in the laboratory, the samples were dried in a convection oven at 50 °C for 42 to 72 h and once dry, they were ground in an agate mortar until they reached a fine powder consistency.

Total elemental concentrations were measured by X-ray fluorescence (XRF), using a portable DELTA model Premium XRF analyzer (hereon referred to as pXRF), with its software in geochemical mode. The pXRF scanner measures elemental composition of the sediment samples as intensities in terms of counts (total or per second) that are proportional to chemical concentrations. Dry and homogenized samples were used to reduce interferences produced by physical variations and sample inhomogeneities and because water content strongly reduce elemental intensities, at least for lighter elements like Si and Al (Tjallingii et al., 2007). The dry sample was placed in a Chemplex® 1900 series plastic container whose lower orifice was covered with a circular (6.3 cm in diameter and 3.6 μm thickness) Mylar® polyester film (Mejía-Piña et al., 2016). The polyester film was held in place with the help of a plastic ring, which crated a taut wrinkle-free sample support window. The upper orifice was then covered with the same type of Mylar® polyester plastic held in place with a second plastic ring, tapping the container several times to obtain a flat surface of the powdery sample in contact with the lower window (Mejía-Piña et al., 2016). The approximate thickness of the sample in the container was ≥0.5 cm. Next, the pXRF unit was placed face up and kept in place with the aid of pieces of foam, positioning the sample container over the analysis window of the instrument.

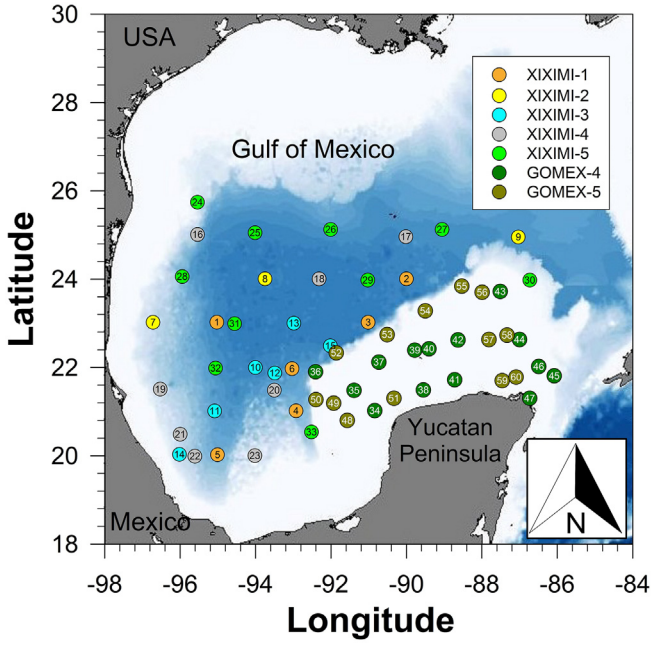

Fig. 1. Map showing the location of sampling sites where surficial sediment was collected from the deep (>1200 m) Gulf of Mexico sea floor, and from the shelf and slope of the Yucatán Peninsula (<230 m depth), during cruises XIXIMI-1 to XIXIMI-5 and GOMEX-4 to GOMEX-5, respectively. The station number is indicated within each symbol.

The pXRF uses two excitation X-ray beams whose duration can be modified based on particular analytical requirements, which in our case required a time of 180 s for each beam, for a total reading time of 360 s. This exposure time was selected as the best for multielemental measurements, following the recommendation of Mejía-Piña et al. (2016). The measured diameter of the X-ray beams for our instrument has a mean value of 6.25 ± 0.55 mm, equivalent to an area of 30.68 ± 0.24 mm^2 (Arenas-Islas et al., 2019). Calibration and measurements of collected samples by the pXRF followed the procedure recommended by Mejía-Piña et al. (2016), using a total of 33 certified reference materials and internal standards. To minimize potential matrix effects produced by our samples, four marine sediments (PACS-2, MESS-3, HISS-1, BCSS-1) from the National Research Council of Canada, two (ES-1646a, NIST-2702) from the National Institute of Standards and Technology, and 12 internal standards involving marine sediments were included in the calibration curve. Instrument readings are quite stable considering that measurements from seven different calibrations were carried out for over two years and varied, on average, 2.5% ± 2.7% (25 standards), 2.7% ± 1.8% (19 standards) and 2.4% ± 1.6% (10 standards) for Al, Ca and Ti, respectively.

For the specific case of surficial sediments from the continental shelf of Yucatán, which contain high $CaCO_3$ concentrations, the calibration curve was constructed using solid mixtures of certified reference material PACS-3 (National Research Council, Halifax, Canada) and an analytical $CaCO_3$ reagent (Mallinckrodt Lab Guard, lot 4072) as a diluent (Arenas-Islas et al., 2019). A total of 11 solid gravimetric mixtures containing 100 to 0% $CaCO_3$ were prepared at successive 10% intervals, until 100% of PACS-3 was attained. In the present study, only the concentrations of three [Al, calcium (Ca), and titanium (Ti)] out of the 27 elements that can be simultaneously analyzed with the pXRF were used. The calibration curves for each element were always highly significant ($P \leq 0.001$), with correlation coefficients (r) in the range 0.965 to 0.971 for Al, 0.943 to 0.957 for Ca, and 0.991 to 0.994 for Ti. The detection limit for each of these elements was calculated as 3× the standard deviation of the average of all the standard deviations obtained from measurements used to construct each calibration curve (Kalnicky and Singhvi, 2001). The detection limits obtained ranged from 8.8 to 9.4, 4.6 to 5.3, and 0.33 to 0.37 μmol g^{-1} for Al, Ca and Ti, respectively. Seventeen of the 27 samples from the Yucatán continental shelf showed total Al concentrations below the detection limit of the XRF. These 17 samples were processed following the method of Carignan and Tessier (1988), which involves the hot, sequential digestion of 0.5 g dry weight of sediment with concentrated acids. The sample is digested in Teflon® beakers with 15 mL of HNO_3 for 30 min at 150 °C under reflux and then evaporated to dryness at 200 °C. Next, 4 mL of $HClO_4$ is added to the sample and heated under reflux during 30 min. The sample is then allowed to cool down (~30 min) followed by addition of 10 mL of HF and evaporation to dryness at 200 °C. Finally, the beaker is rinsed with 5% HCl and the resulting solution is transferred to 50-mL volumetric flasks. Total aluminum concentrations (Al_{tot}) were measured by atomic absorption spectrophotometry (Varian model 240AA), with a detection limit of 1.7 μmol g^{-1}. The certified reference material PACS-3 (National Research Council of Canada) was used to ascertain the accuracy and precision of the Al_{tot} measurements, with a mean recovery percentage of 91.3% and a precision of 1.2%.

Comparison of Al analysis of 686 samples from 33 cores from the deep Gulf of Mexico measured by pXRF (Al_{XRF}) and atomic absorption spectrophotometry (Al_{AAS}), showed that the two groups were statistically similar

(Wilcoxon-Mann-Whitney Rank Sum test, $P = 0.099$). Additionally, a linear regression analysis between Al_{XRF} and Al_{AAS} produced an equation with a slope close to unity [$Al_{XRF} = (0.9728 \pm 0.0055)^{*}Al_{AAS}$, $r = 0.99$, $P < 0.001$]. No statistical analyses were carried out for Ca and Ti because measurements of these two elements by AAS or any other independent analytical method were not available for our samples.

Inorganic (C_i) and total (C_t) carbon concentrations in sediments were determined with a coulometer (UIC, Inc. model CM150) equipped with acidification and combustion modules. For the determination of C_i, ~25 mg of sample was treated in the acidification module, adding 5 mL of 2 N perchloric acid ($HClO_4$) to obtain $CO_{2(g)}$. In the case of C_t, ~20 mg of the sample was introduced into the combustion module at a temperature of 930 °C in an oxygen-rich environment. The $CO_{2(g)}$ generated in both modules was delivered to the electrochemical cell of the coulometer for its quantification. Organic carbon concentrations were calculated by subtracting C_i from C_t. Although the CO_2 coulometer does not require calibration, a standard of $CaCO_3$ powder (Mallinckrodt® 4072) was used, with recoveries of 97.6 ± 2.8% SD ($n = 7$) and 98.9 ± 1.5% ($n = 7$) for C_i and C_t, respectively. Blanks were always below the detection limit of the method (7.3×10^{-4} mmol g^{-1}). Finally, statistical analysis of the data, including Student *t*-tests and fitted linear and exponential functions, was conducted using Excel® and Sigmaplot® software.

This study is based on the hypothesis that $CaCO_3$ concentrations can be estimated by measuring the total Ca concentrations in sediments by XRF. However, it is important to consider that not all the Ca present in sediments occurs as $CaCO_3$, since a major portion can be found associated with lithogenic minerals such as plagioclases ((Ca,Na)(Al,Si)$AlSi_2O_8$), pyroxenes ($Ca_2Si_2O_6$, $Ca_2Mg_5Si_8O_{22}(OH)_2$), and amphiboles ($Ca_2(Mg,Fe)_5Si_8O_{22}(OH)_2$), (10–15%, 3–18% and 10–35%, respectively; Runge, 1966; Li and Schoonmaker, 2005; Wallmann et al., 2008; Haldar and Tišljar, 2014). An alternative to determine the $CaCO_3$ is to calculate the fraction of Ca concentration in the authigenic portion of the sediments (i.e., calcite, aragonite), without considering the lithogenic component.

The concentration of authigenic calcium (Ca_{auth}) can be calculated using the equation proposed by Morford and Emerson (1999):

$$Ca_{auth} = \left(Ca_{tot} - \left(\frac{Ca_{tot}}{Al_{tot}} \right)_{bkg} \times Al_{tot} \right) = Ca_{tot} - Ca_{lith}, \quad (1)$$

where the concentrations of Ca_{tot} and Al_{tot} represent those obtained by XRF or AAS analyses, whereas $(Ca_{tot}/Al_{tot})_{bkg}$ represents the Ca:Al ratio of their background concentrations. For this study, the Earth's crust values reported by Turekian and Wedepohl (1961) and Li and Schoonmaker (2005) were used as reference values. Eq. (1) calculates Ca_{auth} by estimating the concentration of lithogenic Ca (Ca_{lith}) of a given sediment, based on its Al concentration and assuming that its background concentrations follow the ratio Ca_{tot}/Al_{tot} of the Earth's crust. Geochemical normalization is generally accomplished by using Al, a conservative element that is part of the structure of clays and, therefore, can be considered as one of the best proxies to represent clay mineral concentration (Kersten and Smedes, 2002). Additionally, Al is not likely to be significantly affected by anthropogenic sources and is the second most abundant element in the earth's crust (Schropp et al., 1990). Furthermore, crustal average values have long been used as cutoffs for authigenic enrichment in sediments (e.g., de Groot et al., 1982; Schropp et al., 1990; Morford and Emerson, 1999; Tribovillard et al., 2013; Reinhard et al., 2014; Zhang et al., 2016; Cole et al., 2017). The choice of using crustal abundances is because fine-grained shales, which constitutes up to 70% of the stratigraphic record, dominate the sedimentary record (Garrels and Mackenzie, 1971) and because most trace elements are enriched in shales compared to other sediment constituents (McLennan, 2001). The difference between measured Ca_{tot} and calculated Ca_{lith} represents the fraction of authigenic Ca present in the sample. If the Ca_{auth} effectively represents $CaCO_3$, then there are two ways to quantify the concentrations of this mineral in aquatic sediments. The first is simply to assume and demonstrate that the Ca_{auth} concentrations are statistically equivalent to those of $CaCO_3$. The second approach involves measuring C_i concentrations by any of the techniques described in the Introduction, and then compares them with the Ca_{auth} values through a linear regression analysis. The validity of both approximations based on the results obtained is discussed below.

4. Results

Overall, surficial inorganic carbon (C_i) values, expressed in mmol g^{-1} (% of $CaCO_3$), ranged from 1.89 (18.9%) to 9.66 (96.7%) for samples X5–11 and G4-G33, respectively, and averaged 6.0 ± 3.0 mmol g^{-1} (60 ± 31%) for the 60 analyzed samples. The mean value of Ca_{auth} was 5.4 ± 3.0 mmol g^{-1} (55 ± 30%), with a range of 1.33 to 9.07 mmol g^{-1} (13.3 to 90.8%) for samples X4–45 and G5-N66, respectively. In the specific case of deep Gulf of Mexico sediments, the mean C_i concentration (Table S3) was 3.4 ± 1.3 mmol g^{-1} (35 ± 13%), whereas the range was 1.91 to 7.41 mmol g^{-1} (19.2% to 74.2%) for samples X1–40 y X5–18, respectively. Values of Ca_{auth} (Table S3) in deep sediments ranged from 1.33 to 7.41 mmol g^{-1} (13.3% to 74.2%), averaging 2.9 ± 1.3 mmol g^{-1} (29 ± 13%). In the case of shelf and slope sediments of the Yucatan Peninsula (Table S4), the C_i values were far greater, with a mean value of 9.17 ± 0.54 mmol g^{-1} (91.8 ± 5.4%) and a range of 6.69 to 9.66 mmol g^{-1} (67.0 to 96.6%) for stations G4-C15 and G4-G33, respectively, while Ca_{auth} values (Table S4) ranged from 6.14 to 90.8 mmol g^{-1} (61.4 to 90.8%) for stations G4-C15 and G5-N66, respectively, and averaged 8.53 ± 0.53 mmol g^{-1} (85.4 ± 5.3%).

Our results show that there is a general C_i and Ca_{auth} spatial pattern in the southern Gulf of Mexico (Fig. 2), with high values along the Yucatan continental shelf in the east (<230 m depth) and low concentrations in the western side of the Gulf (>1200 m depth). This east to west gradient for the southern Gulf of Mexico is probably the result of several sources of sedimentary material and transport processes. The continental shelf of the Gulf reflects nearby sources of terrigenous material or autochthonous carbonate sediments, with Campeche Bay marking the transition from terrigenous to carbonates (Davis, 2017). One of the main sources of the terrigenous contribution are the Grijalva-Usumacinta and San Pedro-San Pablo rivers located in northeast Mexico (Diaz-Asencio et al., 2019). This delta system accounts for 35% of the total drainage of Mexico and represents its largest deltaic fluvial system (Arana et al., 2005). Calcium carbonate is mostly found in shallow water and is abundant in the Yucatan Peninsula, with the province of the Campeche shelf contributing intrabasinal carbonates to the abyssal plain of the Gulf (Davies, 1972). Hence, Fig. 2 suggests that once on the continental shelf, fine terrigenous and carbonate materials are dispersed and redeposited, probably by currents, wind waves, storm waves and tidal currents, as has been reported for several carbonate-terrigenous transitions (e.g., Holmes and Evans, 1963; Roberts, 1987; Gillespie and Nelson, 1996; Brandano and Civitelli, 2007; Francis et al., 2007). Subsequently, these materials are further transported and deposited in the abyssal area of the Gulf of Mexico by differential pelagic settling, turbidity currents and bottom currents (Davies, 1972). However, it is important to emphasize that the mechanisms for transporting terrigenous and carbonate materials to the abyssal plain of the Gulf of Mexico remain poorly understood.

5. Discussion

5.1. Authigenic calcium

To evaluate the reliability of these measurements, the spatial distribution of Ca_{auth} concentrations obtained with the pXRF was compared with those of C_i measured by coulometry and, as observed in Fig. 2, both distributions were very similar. In both cases the highest $CaCO_3$ concentrations (>8 mmol g^{-1}) were observed in the Yucatán

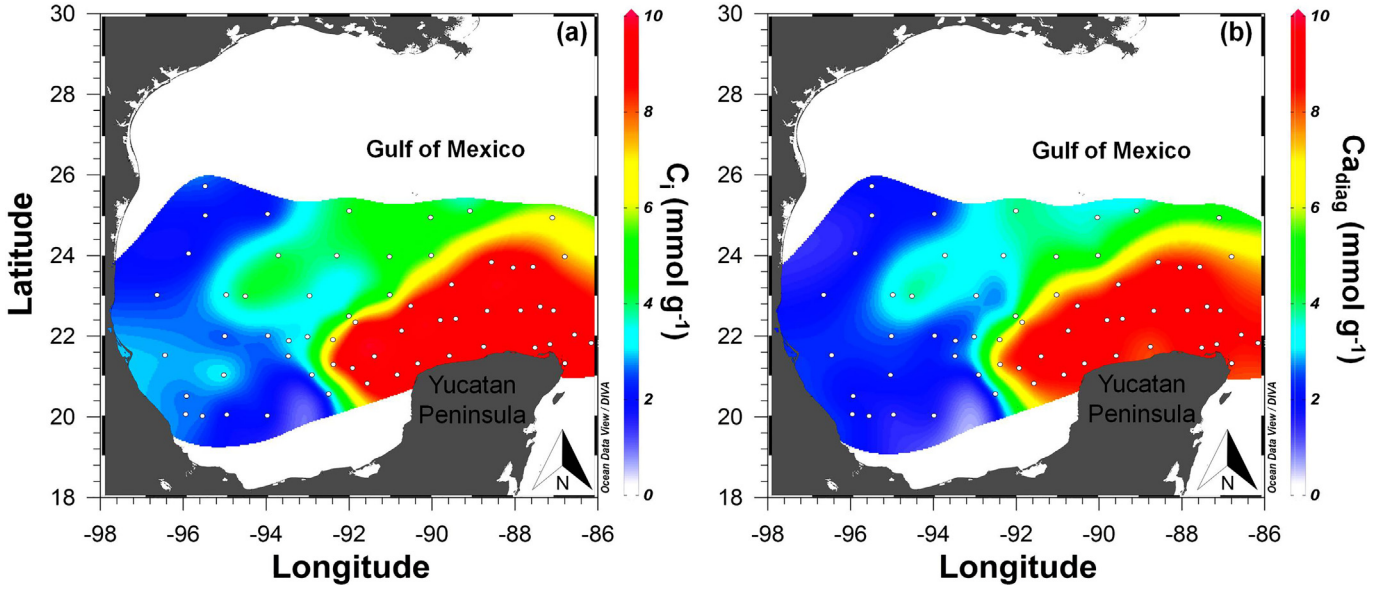

Fig. 2. Spatial distribution of (a) inorganic carbon (C_i), and (b) authigenic calcium (Ca_{auth}) in surficial sediments of the Gulf of Mexico, and the shelf and slope of the Yucatán Peninsula (white circles indicate sampling stations).

continental shelf, and the lowest (<3 mmol g^{-1}) in the areas near the western coast of the Gulf of Mexico (possibly due to the dilution effect of the input of terrigenous components from the adjacent continental mass), with intermediate concentrations in the deepest portion of the Gulf. Slight differences between the two distributions may be attributed to the omission of other carbonates unrelated to Ca, as described below. It is noteworthy that the means (Gulf of Mexico and shelf and slope of the Yucatan Peninsula combined) obtained for C_i and Ca_{auth} were statistically similar ($t_{Student}$ test, $P = 0.2756$, $n = 60$), allowing establishment of the reliability of the values obtained with the pXRF (first approximation). Furthermore, average offsets between C_i and Ca_{auth} were relatively small: 11.7% ± 9.0% for all the samples combined ($n = 60$), 16% ± 10% for the deepest portion of the Gulf ($n = 33$), and 7.0% ± 3.3% for the Yucatán continental shelf ($n = 27$).

For the second approximation, Ca_{auth} concentrations were compared with those of C_i determined by coulometry. A simple linear regression was fitted to the data (in mmol g^{-1}):

$$Ca_{auth} = (0.972 \pm 0.014) * C_i - (0.403 \pm 0.093);\ r = 0.99;\ P0.001;\ n = 60 \quad (2)$$

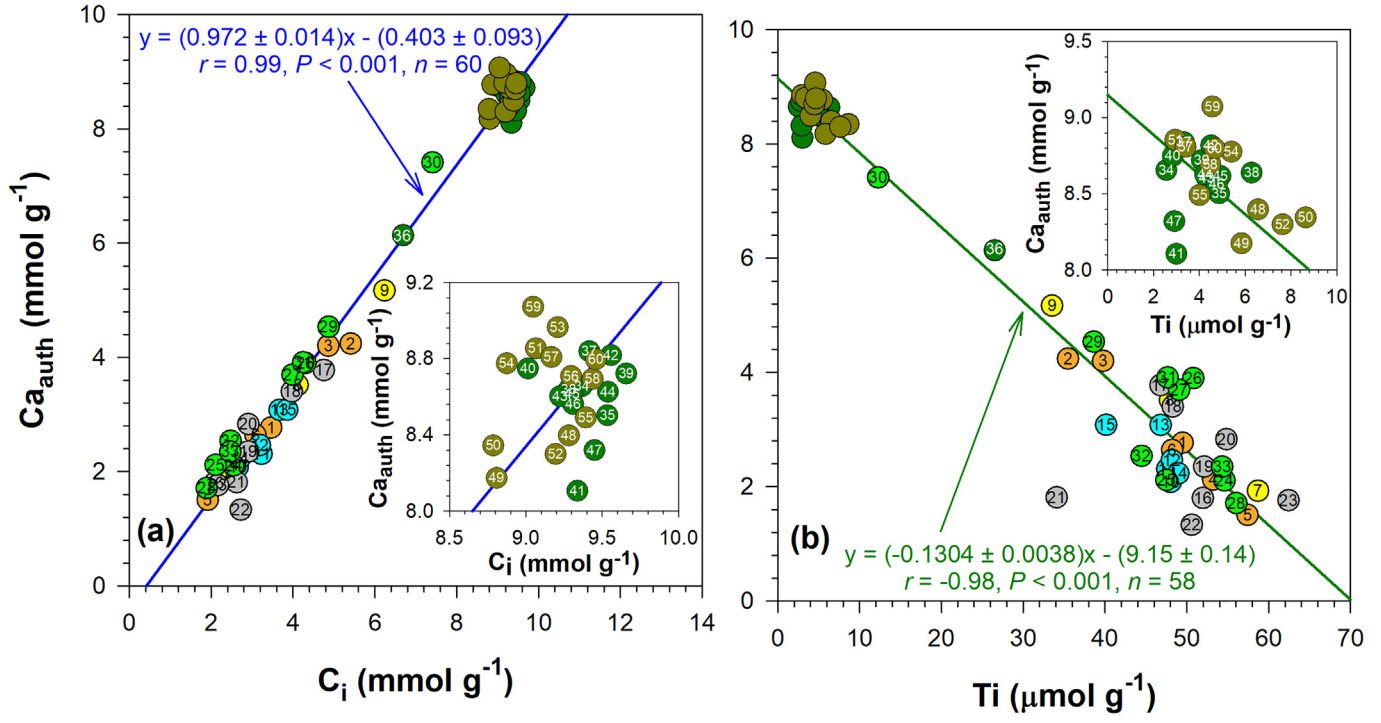

Fig. 3. Relationship between the concentrations of (a) authigenic calcium (Ca_{auth}) and inorganic carbon (C_i), and (b) those of Ca_{auth} and titanium (Ti) in surficial sediments of the Gulf of Mexico, and the shelf and slope of the Yucatán Peninsula. The blue and green lines in (a) and (b), respectively, represent the fitted linear regressions between the variables, and their corresponding equations (symbols as in Fig. 1). Inserts represent the relationship between these variables, but with expanded scales. (For interpretation of the references to colour in this figure legend, the reader is referred to the web version of this article.)

This equation showed a slope close to unity with a small associated standard error (SE) of 1.4% and a Y-intercept very close to zero (-0.403 ± 0.093 SE; Fig. 3a). It is noteworthy that Ca_{auth} values should be slightly lower than those of C_i, since analysis by coulometry includes other carbonates unrelated to Ca (e.g., $MgCO_3$, $SrCO_3$, $MnCO_3$, $FeCO_3$; Goldberg and Arrhenius, 1958; Aller and Rude, 1988; Morse, 2003), and that the negative Y-intercept in Eq. (2) suggests precisely this behavior. Furthermore, this equation may explain our previously calculated average offset values obtained between C_i and Ca_{auth}. No attempt was made to calculate the relative contributions of authigenic Mg, Mn and Fe to Ca_{auth}, since Mg was detected by the pXRF in only a few samples and Mn and Fe are mostly associated to oxyhydroxides. Only Sr was consistently detected by the pXRF, but the contribution of its authigenic fraction to the carbonate pool was too low (range of 0.17% to 0.86% and mean of 0.34% ± 0.16%) to significantly modify the parameters of Eq. (2). Thus, several sediment samples measured by coulometry (or other reliable method) can be used to apply this method to aquatic sediments and calibrate Ca_{auth} with Ca values measured with the pXRF. From the linear regression obtained from plotting C_i vs. Ca_{auth}, it is now possible to calculate C_i in other samples using the equation:

$$C_i = \frac{Ca_{auth} + a}{m}, \quad (3)$$

where *a* and *m* represent the Y-intercept and slope of the linear regression (e.g., Eq. (2)), respectively.

The procedure described in this work can be applied to different sedimentary settings to obtain meaningful results, as long as a C_i vs. Ca_{auth} calibration curve is constructed for each setting. It is not recommended to use the same slope and intercept values that were obtained in our Eq. (2), since each pXRF has different instrumental characteristics that, most probably, will modify these parameters. Additionally, strict calibration procedures (e.g., Mejía-Piña et al., 2016; Arenas-Islas et al., 2019) must be followed so that Ca and Al concentrations are accurately measured. Finally, matrix effects produced by different rocks and sediment textures could affect the pXRF measurements in ways that at this point are not possible to predict, especially when in situ measurements are carried out.

5.2. Calcium carbonate and titanium

One of the advantages of the method proposed in this study is that the pXRF allows simultaneous measurement of the total concentration of other elements, which can provide valuable additional information about the sedimentary system undergoing analysis. For example, Ti provides one of the best proxies of terrigenous contributions to marine sediments (Applebaum and Bouma, 1972; Schroeder et al., 1997; Wei et al., 2003; Hennekam and de Lange, 2012; Celis-Hernandez et al., 2018). There is a highly significant inverse correlation between this element and Ca_{auth} for Gulf of Mexico and Yucatan Peninsula shelf and slope samples combined ($P \leq 0.001$, $r = -0.98$, $n = 58$; Fig. 3b). Fig. 3 shows that surficial shelf and slope carbonate sediments of the Yucatan Peninsula represent one end member of the Ca_{auth}:Ti ratio, indicating that these sediments clearly influence the spatial distribution of carbonates in deep part of the Gulf of Mexico (e.g., Fig. 2). In addition, these results reveal that carbonates and terrigenous materials are gradually mixed spatially (e.g., Hays and Perruzza, 1972; Ingram et al., 2010). Gradual mixing of these two sedimentary components has been previously reported for sediments of North Queensland margin of Australia (Francis et al., 2007), pelagic western Mediterranean Sea (Hoogakker et al., 2004), and Campeche Bank and Bay region of the Gulf of Mexico (Arana et al., 2005). Mount (1984) divided the processes responsible for the mixing of carbonates and terrigenous sediments into four categories: (1) punctuated mixing, when sediments are transferred from one depositional environment to another by sporadic storms and other extreme periodic events; (2) facies mixing, where mixing of sediments occur along diffuse boundaries between contrasting facies; (3) in situ mixing, where autochthonous or parautochthonous death assemblages of calcareous organisms form the carbonate fraction accumulating on or within siliciclastic substrates; and (4) source mixing, where admixtures are formed by the uplift and erosion of nearby carbonate source terranes. According to this author, the Eastern Gulf of Mexico can be classified as a facies mixing setting, where

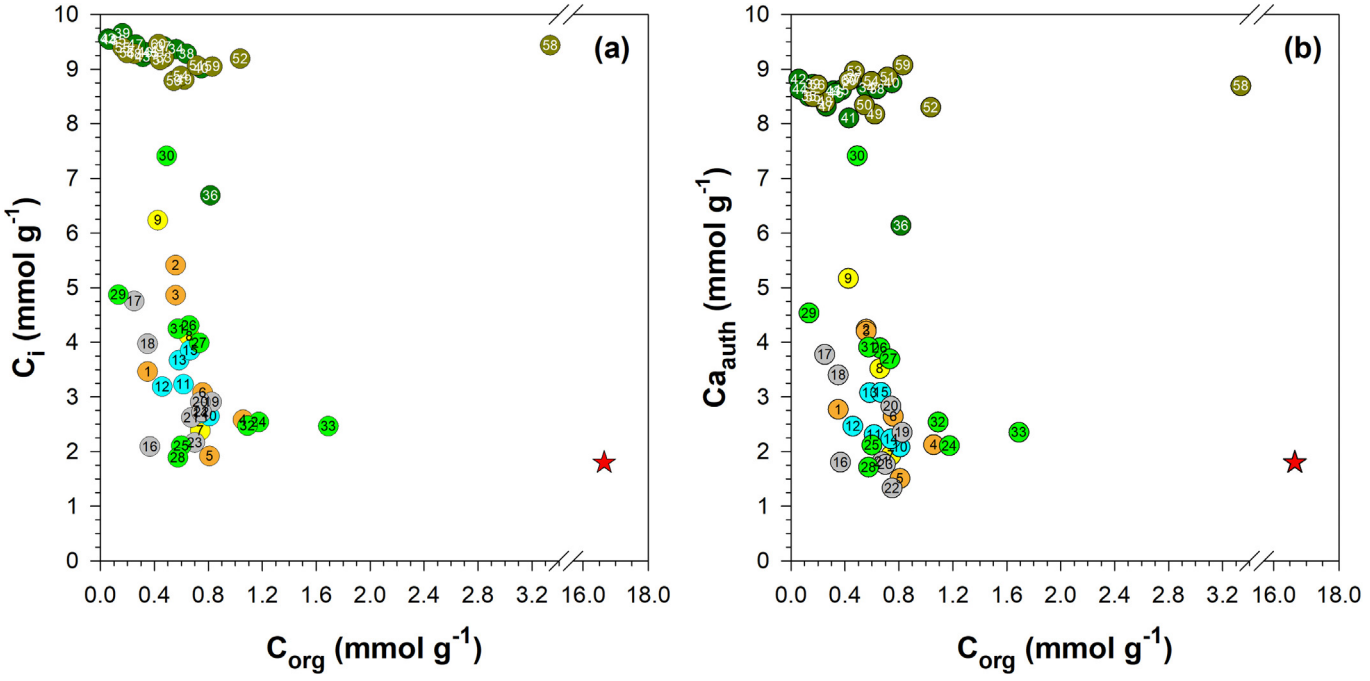

Fig. 4. Concentrations of (a) organic carbon (C_{org}) vs. inorganic carbon (C_i), and (b) C_{org} vs. authigenic calcium (Ca_{auth}) in surficial sediments of the Gulf of Mexico. The red star indicates the C_i and C_{org} values reported by Orcutt et al. (2010) for a hydrocarbon seep site in the Gulf of Mexico (symbols as in Fig. 1). (For interpretation of the references to colour in this figure legend, the reader is referred to the web version of this article.)

sediments are mixed along the diffuse boundaries between contrasting facies. Our results (Fig. 3b) and those of Arana et al. (2005) for the Campeche Bank and Bay suggest that this classification most probably can be extended to the entire southern Gulf of Mexico. Present-day examples of facies mixing can be found in northeast Australia (Dunbar and Dickens, 2003), New Zealand (James et al., 2001), Belize (Ferro et al., 1999), and the Pontine Islands in the Tyrrhenian Sea (Brandano and Civitelli, 2007).

Studies on terrigenous-carbonate transitions studies are important because they can provide critical information about processes influencing different types of carbonate and siliciclastic depositions, which can be used in hydrocarbon exploration (e.g., Roberts and Murray, 1988). Furthermore, our results may provide a modern analog for interpreting ancient sedimentary sequences. Finally, it is important to mention that understanding the transport mechanisms of terrigenous and carbonate sediments in the southern Gulf of Mexico should remain as an important topic of research.

5.3. Inorganic carbon, authigenic calcium and organic carbon

Plots of C_{org} vs. C_i and C_{org} vs. Ca_{auth} for Gulf of Mexico surficial sediment samples showed very similar behaviors (Fig. 4), suggesting that the Ca_{auth} values can be reliably used instead of C_i values. This figure also shows the presence of two groups: (1) samples from the shelf and slope of the Yucatan Peninsula, with a relatively wide range of C_{org} values (0.057–1.0 mmol g^{-1}), and high C_i and Ca_{auth} concentrations that are within a narrow range of values (8.8–9.7 and 8.1–9.1 mmol g^{-1}, respectively); and (2) samples from the deep sediments of the Gulf of Mexico, with a wide range of C_{org} (0.13–1.7 mmol g^{-1}) and C_i and Ca_{auth} values (1.9–7.4 and 1.3–7.4 mmol g^{-1}, respectively). There are two samples from the shelf and slope of the Yucatan Peninsula, however, that show high C_{org} (G5-M63) and low C_i and Ca_{auth} (G4-C15) values (Table S4), but the general overall trend is for the sediments to decrease their C_i (or Ca_{auth}) concentrations as the C_{org} values increase (Fig. 4). Hence, Fig. 4 shows that there are two end members: one represented by sediments with high C_i (Ca_{auth}) values and low concentrations of C_{org}, and the other by sediments with high C_{org} content and low C_i (Ca_{auth}) values. In the first case, the sedimentary environment is represented by sample G4-J48 collected in the shelf and slope of the Yucatan Peninsula (Table S4), while the second case corresponds to station X5–44 (Table S3), which may be influenced by natural hydrocarbon seeps that make a major contribution to the amount of C_{org} in the sediment. This assumption is based on the proximity of this station to hydrocarbon seeps (MacDonald et al., 2004; Ding et al., 2008; Brüning et al., 2010), whose sediments are characterized by high C_{org} concentrations (e.g., 16.7 mmol g^{-1}; Fig. 4) (Orcutt et al., 2010). The decrease of the C_i (Ca_{auth}) values with increasing C_{org} shown in Fig. 4, may result from the combined effects of carbonate dilution by material of terrigenous origin, and by the increasing incorporation of organic matter (biogenic and contributed by hydrocarbons) to the sediments. The former is clearly observed in Fig. 3b, where Ca_{auth} decreases linearly with increasing Ti concentrations. The second process can be inferred from the results obtained for sediments of the Yucatán continental shelf. In this case, the increase in C_{org} concentrations appears to be responsible for the decrease in C_i (Ca_{auth}) values (Fig. 4), since $CaCO_3$ concentrations are relatively constant in shelf and slope sediments of the Yucatan Peninsula sediments (92.5 ± 5.5% SD). In the extreme case of the hydrocarbon seeps, carbonates that are present as an outcrop are extensively diluted by seeping hydrocarbons, a process that generates extremely high C_{org} values (Fig. 4) (Orcutt et al., 2010).

6. Conclusions

A non-destructive, rapid, low cost and reliable method was developed to calculate authigenic Ca (Ca_{auth}), used as a proxy of $CaCO_3$ concentrations in sediments, with a portable X-ray fluorescence instrument (pXRF). An added advantage of this technique is that up to 27 elements can be simultaneously measured in the same sample, some of which can be used to complement geochemical studies of carbonate sedimentary systems. To improve the accuracy of the measurements, it is highly recommended to calibrate the method with independent inorganic carbon measurements, since deviations from the actual values can be obtained from the contributions of other sedimentary carbonates (e.g., $MgCO_3$, $SrCO_3$, $MnCO_3$, $FeCO_3$) that are not included in the Ca_{auth} calculations. Evaluation of our calibration results showed a highly significant ($P < 0.001$, $r = 0.99$) linear regression between C_i and Ca_{auth} concentrations, as well as statistically similar values between these two variables. Application of the new method to deep (>1200 m water depth) and shallow (<230 m) samples of the Gulf of Mexico and Yucatan Peninsula shelf and slope, respectively, showed a west to east gradient of increasing $CaCO_3$ concentrations. This gradient is the consequence of a gradual mixing of terrigenous and carbonate sediments along the southern Gulf of Mexico, as suggested by the inverse relationship obtained between Ti and Ca_{auth}. Finally, another mixing process that is probably underway is between carbonates and organic carbon in Gulf of Mexico sediments, as suggested by the combined behavior of these two sedimentary components.

Supplementary data to this article can be found online at https://doi.org/10.1016/j.sedgeo.2020.105724.

Declaration of competing interest

The authors declare that they have no known competing financial interests or personal relationships that could have appeared to influence the work reported in this paper.

Acknowledgments

The authors thank the crew of the oceanographic vessel Justo Sierra for their help in sample collection, and Virginia Martínez, Gabriela Cervantes, Alexandro Orozco and Ramón Martínez for the analysis of samples. This research was supported by the Consejo Nacional de Ciencia y Tecnología (CONACYT) and the Secretariat of Energy, through the Fondo Sectorial CONACYT-Secretaría de Energía-Hidrocarburos, project 201441. This work represents a contribution of the Gulf of Mexico Research Consortium (CIGoM). Support for the graduate and terminal scholarship granted to J.G.O. by CONACYT and CIGoM, respectively, are also greatly appreciated. The authors are indebted to Jasper Knight and one anonymous reviewer for their insightful comments, which improved this article. Declarations of interest: none.

References

Aguayo, J.E., Bello, R., del Vecchio, M.A., Araujo, J., Basáñez, M.A., 1980. Estudio sedimentológico en el área Tulum-Cancún-Isla Mujeres, Estado de Quintana Roo, México. Bol. Soc. Geol. Mex. 41, 15–32.

Aller, R.C., Rude, P.D., 1988. Complete oxidation of solid phase sulfides by manganese and bacteria in anoxic marine sediments. Geochim. Cosmochim. Acta 52, 751–765.

Anbu, P., Kang, C., Shin, Y., So, J., 2016. Formations of calcium carbonate minerals by bacteria and its multiple applications. Springerplus 5, 250. https://doi.org/10.1186/s40064-016-1869-2.

Andrade, S., Ulbrich, H.H., Janasi, V.A., Navarro, M.S., 2009. The determination of total hydrogen, carbon, nitrogen and sulfur in silicates, silicate rocks, soils and sediments. Geostand. Geoanal. Res. 33, 337–345.

Applebaum, B.S., Bouma, A.H., 1972. Geology of upper continental slope in alaminos Canyon region. AAPG Bull. 56, 1895–1896.

Arana, H.A.H., Attrill, M.J., Hartley, R., Bouchot, G.G., 2005. Transitional carbonate-terrigenous shelf sub-environments inferred from textural characteristics of surficial sediments in the Southern Gulf of Mexico. Cont. Shelf Res. 25, 1836–1852.

Archer, D., Maier-Reimer, E., 1994. Effect of deep-sea sedimentary calcite preservation on atmospheric CO_2 concentration. Nature 367, 260–263.

Arenas-Islas, D., Huerta-Diaz, M.A., Norzagaray-López, C.O., Mejía-Piña, K.G., Otero, X.L., Valdivieso-Ojeda, J.A., Árcega-Cabrera, F., 2019. Calibration of a handheld X-ray fluorescence equipment for geochemical analysis of samples with carbonated matrices. Sediment. Geol. 391, 105517. https://doi.org/10.1016/j.sedgeo.2019.105517.

Arne, D.C., Mackie, R.A., Jones, S.A., 2014. The use of property-scale portable X-ray fluorescence data in gold exploration: advantages and limitations. Geochem. Explor. Environ. Anal. 14, 233–244.

Balsam, W.L., Beeson, J.P., 2003. Sea-floor sediment distribution in the Gulf of Mexico. Deep-Sea Res. I 50, 1421–1444.

Ben-Yaakov, S., Ruth, E., Kaplan, I.R., 1974. Carbonate compensation depth: relation to carbonate solubility in ocean waters. Science 184, 982–984.

Blatt, H., Middleton, G., Murray, R., 1980. Origin of Sedimentary Rocks. Prentice-Hall, New Jersey 782 p.

Brandano, M., Civitelli, G., 2007. Non-seagrass meadow sedimentary facies of the Pontinian Islands, Tyrrhenian Sea: a modern example of mixed carbonate-siliciclastic sedimentation. Sediment. Geol. 201, 286–301.

Broecker, W.S., Peng, T.-H., 1987. The role of $CaCO_3$ compensation in the glacial to interglacial atmospheric CO_2 change. Glob. Biogeochem. Cycles 1, 15–29.

Brüning, M., Sahling, H., MacDonald, I.R., Ding, F., Bohrmann, G., 2010. Origin, distribution, and alteration of asphalts at Chapopote Knoll, Southern Gulf of Mexico. Mar. Petrol. Geol. 27, 1093–1106.

Carignan, R., Tessier, A., 1988. The co-diagenesis of sulfur and iron in acid lake sediments of southwestern Québec. Geochim. Cosmochim. Acta 52, 1179–1188.

Celis-Hernandez, O., Rosales-Hoz, L., Cundy, A.B., Carranza-Edwards, A., Croudace, I.W., Hernandez-Hernandez, H., 2018. Historical trace element accumulation in marine sediments from the Tamaulipas shelf, Gulf of Mexico: an assessment of natural vs anthropogenic inputs. Sci. Total Environ. 622, 325–336.

Cole, D.B., Zhang, S., Planavsky, N.J., 2017. A new estimate of detrital redox-sensitive metal concentrations and variability in fluxes to marine sediments. Geochim. Cosmochim. Acta 215, 337–353.

Crupi, V., Giunta, A., Kellett, B., Longo, F., Maisano, G., Majolino, D., Scherillo, A., Venuti, V., 2014. Handheld and non-destructive methodologies for the compositional investigation of meteorite fragments. Anal. Methods 6, 6301–6309.

Dahl, T.W., Ruhl, M., Hammarlund, E.U., Canfield, D.E., Rosing, M.T., Bjerrum, C.J., 2013. Tracing euxinia by molybdenum concentrations in sediments using handheld X-ray fluorescence spectroscopy (HHXRF). Chem. Geol. 360/361, 241–251.

Davies, D.K., 1972. Deep sea sediments and their sedimentation, Gulf of Mexico. AAPG Bull. 56, 2212–2239.

Davies, D.K., Moore, W.R., 1970. Dispersal of Mississippi sediment in the Gulf of Mexico. J. Sediment. Petrol. 40, 339–353.

Davis, R.A., 2017. Sediments of the Gulf of Mexico. In: Ward, C. (Ed.), Habitats and Biota of the Gulf of Mexico: Before the Deepwater Horizon Oil Spill. Springer, New York, pp. 165–215.

de Groot, A., Zshuppe, K., Salomons, W., 1982. Standardization of methods of analysis for heavy metals in sediments. Hydrobiology 92, 689–695.

de Winter, N.J., Claeys, P., 2017. Micro X-ray fluorescence (μXRF) line scanning on Cretaceous rudist bivalves: a new method for reproducible trace element profiles in bivalve calcite. Sedimentology 64, 231–251.

de Winter, N.J., Sinnesael, M., Makarona, C., Vansteenberge, S., Claeys, P., 2017. Trace element analyses of carbonates using portable and micro-X-ray fluorescence: performance and optimization of measurement parameters and strategies. J. Anal. At. Spectrom. 32, 1211–1223.

Dean, W.E., 1974. Determination of carbonate and organic matter in calcareous sediments and sedimentary rocks by loss on ignition: comparison with other methods. J. Sediment. Petrol. 44, 242–248.

D'Elia, M., Blanco, A., Galiano, A., Orfino, V., Fonti, S., Mancarella, F., Guido, A., 2016. A comparative SEM morphological study of biogenic and abiogenic carbonates for the search for biostructures on Mars. Mem. Soc. Astron. Ital. 87, 97–103.

Diaz-Asencio, M., Ferreira Bartrina, V., Herguera, J.C., 2019. Sediment accumulation patterns on the slopes and abyssal plain of the southern Gulf of Mexico. Deep-Sea Res. I 146, 11–23.

Ding, F., Spiess, V., Brüning, M., Fekete, N., Keil, H., Bohrmann, G., 2008. A conceptual model for hydrocarbon accumulation and seepage processes around Chapopote asphalt site, southern Gulf of Mexico: from high resolution seismic point of view. J. Geophys. Res. Solid Earth 113B, 08404. https://doi.org/10.1029/2007JB005484.

Dunbar, G.B., Dickens, G.R., 2003. Massive siliciclastic discharge to slopes of the Great Barrier Reef Platform during sea-level transgression: constraints from sediment cores between 15°S and 16°S latitude and possible explanations. Sediment. Geol. 162, 141–158.

Engleman, E.E., Jackson, L.L., Norton, D.R., 1985. Determination of carbonate carbon in geological materials by coulometric titration. Chem. Geol. 53, 125–128.

Falkowski, P., Scholes, R.J., Boyle, E., Canadell, J., Canfield, D., Elser, J., Gruber, N., Hibbard, K., Högberg, P., Linder, S., Mackenzie, F.T., Moore III, B., Pedersen, T., Rosenthal, Y., Seitzinger, S., Smetacek, V., Steffen, W., 2000. The global carbon cycle: a test of our knowledge of Earth as a system. Science 290, 291–296.

Ferro, C.E., Droxler, A.W., Anderson, J.B., Mucciarone, D., 1999. Late Quaternary shift of mixed siliciclastic-carbonate environments induced by glacial eustatic sea-level fluctuations in Belize. In: Harris, P.M., Saller, A.H., Simo, J.A. (Eds.), Advances in Carbonate Sequence Stratigraphy; Application to Reservoirs, Outcrops and Models. SEPM, Special Publication vol. 63, pp. 385–411.

Francis, J.M., Dunbar, G.B., Dickens, G.R., Sutherland, I.A., Droxler, A.W., 2007. Siliciclastic sediment across the North Queensland margin (Australia): a Holocene perspective on reciprocal versus coeval deposition in tropical mixed siliciclastic-carbonate systems. J. Sediment. Res. 77, 572–586.

Garrels, R.M., Mackenzie, F.T., 1971. Evolution of Sedimentary Rocks. W.W. Norton and Co., New York 397 p.

Gillespie, J.L., Nelson, C.S., 1996. Distribution and control of mixed terrigenous-carbonate surficial sediment facies, Wanganui shelf, New Zealand. N. Z. J. Geol. Geophys. 39, 533–549.

Goldberg, E.D., Arrhenius, G.O.S., 1958. Chemistry of Pacific pelagic sediments. Geochim. Cosmochim. Acta 13, 153–212.

Goñi, M.A., Ruttenberg, K.C., Eglinton, T.I., 1997. Sources and contribution of terrigenous organic carbon to surface sediments in the Gulf of Mexico. Nature 389, 275–278.

Haldar, S.K., Tišljar, J., 2014. Introduction to Mineralogy and Petrology. Elsevier, Amsterdam 338 p.

Hays, J.D., Perruzza, A., 1972. The significance of calcium carbonate oscillations in eastern equatorial Atlantic deep-sea sediments for the end of the Holocene warm interval. Quat. Res. 2, 355–362.

Hedges, J.I., Parker, P.L., 1976. Land-derived organic matter in surface sediments from the Gulf of Mexico. Geochim. Cosmochim. Acta 40, 1019–1029.

Heiri, O., Lotter, A.F., Lemcke, G., 2001. Loss on ignition as a method for estimating organic and carbonate content in sediments: reproducibility and comparability of results. J. Paleolimnol. 25, 101–110.

Hennekam, R., de Lange, G., 2012. X-ray fluorescence core scanning of wet marine sediments: methods to improve quality and reproducibility of high-resolution paleoenvironmental records. Limnol. Oceanogr. Methods 10, 991–1003.

Hines, B.R., Gazley, M.F., Collins, K.S., Bland, K.J., Crampton, J.S., Ventura, G.T., 2019. Chemostratigraphic resolution of widespread reducing conditions in the Southwest Pacific Ocean during the Late Paleocene. Chem. Geol. 504, 236–252.

Holmes, C.W., Evans, R.G., 1963. Sedimentology of Gullivan Bay and vicinity, Florida. Sedimentology 2, 189–206.

Hoogakker, B.A.A., Rothwell, R.G., Rohling, E.J., Paterne, M., Stow, D.A.V., Herrle, J.O., Clayton, T., 2004. Variations in terrigenous dilution in western Mediterranean Sea pelagic sediments in response to climate change during the last glacial cycle. Mar. Geol. 211, 21–43.

Huffman, E.W.D., 1977. Performance of a new automatic carbon dioxide coulometer. Microchem. J. 22, 567–573.

Ibañez-Insa, J., Pérez-Cano, J., Fondevilla, V., Oms, O., Rejas, M., Fernández-Turiel, J.L., Anadón, P., 2017. Portable X-ray fluorescence identification of the Cretaceous-Paleogene boundary: application to the Agost and Caravaca sections, SE Spain. Cretac. Res. 78, 139–148.

Ingram, W.C., Meyers, S.R., Brunner, C.A., Martens, C.S., 2010. Late Pleistocene–Holocene sedimentation surrounding an active seafloor gas-hydrate and cold-seep field on the Northern Gulf of Mexico Slope. Mar. Geol. 278, 43–53.

James, N.P., Bone, Y., Collins, L.B., Kyser, T.K., 2001. Surficial sediments of the Great Australian Bight: facies dynamics and oceanography on a vast cool-water carbonate shelf. J. Sediment. Res. 71, 549–567.

Johnson, K.M., King, A.E., Sieburth, J.M., 1985. Coulometric TCO_2 analyses for marine studies; an introduction. Mar. Chem. 16, 61–82.

Johnson, K.M., Sieburth, J.M., Williams, P.J.B., Brandström, L., 1987. Coulometric total carbon dioxide analysis for marine studies: Automation and calibration. Mar. Chem. 21, 117–133.

Kalnicky, D.J., Singhvi, R., 2001. Field portable XRF analysis of environmental samples. J. Hazard. Mater. 83, 93–122.

Kersten, M., Smedes, F., 2002. Normalization procedures for sediment contaminants in spatial and temporal trend monitoring. J. Environ. Monit. 4, 109–115.

Kessler, L., Nagarajan, R., 2012. A semi-quantitative assessment of clay content in sedimentary rocks using portable X-ray fluorescence spectrometry. Int. J. Earth Sci. Eng. 5, 363–364.

Kristensen, E., Andersen, F.Ø., 1987. Determination of organic carbon in marine sediments: a comparison of two CHN-analyzer methods. J. Exp. Mar. Biol. Ecol. 109, 15–23.

Lemiere, B., Laperche, V., Haouche, L., Auger, P., 2014. Portable XRF and wet materials: application to dredged contaminated sediments from waterways. Geochem. Explor. Environ. Anal. 14, 257–264.

Lenton, T.M., Britton, C., 2006. Enhanced carbonate and silicate weathering accelerates recovery from fossil fuel CO_2 perturbations. Glob. Biogeochem. Cycles 20, GB3009. https://doi.org/10.1029/2005GB002678.

Li, Y.-H., Schoonmaker, J.E., 2005. Chemical composition and mineralogy of marine sediments. In: Mackenzie, F.T. (Ed.), Sediments, Diagenesis, and Sedimentary Rocks. vol. 7. Elsevier-Pergamon, Oxford, pp. 1–35.

Logan, B.W., Harding, J.L., Aur, W.M., Williams, J.D., Sneat, R.G., 1969. Carbonate sediments on reefs, Yucatan shelf, Mexico, part I, Late Quaternary sediments. Mem. Am. Assoc. Pet. Geol. 11, 7–128.

MacDonald, I.R., Bohrmann, G., Escobar, E., Abegg, F., Blanchon, P., Blinova, V., Bruckmann, W., Drews, M., Eisenhauer, A., Han, X., Heeschen, K., Meier, F., Mortera, C., Naehr, T., Orcutt, B., Bernard, B., Brooks, J., de Farago, M., 2004. Asphalt volcanism and chemosynthetic life in the Campeche Knolls, Gulf of Mexico. Science 304, 999–1002.

Macreadie, P.E., Serrano, O., Maher, D.T., Duarte, C.M., Beardall, J., 2017. Addressing calcium carbonate cycling in blue carbon accounting. Limnol. Oceanogr. Lett. 2, 195–201.

McLennan, S.M., 2001. Relationships between the trace element composition of sedimentary rocks and upper continental crust. Geochem. Geophys. Geosyst. 2. https://doi.org/10.1029/2000GC000109 2000GC000109.

Mcleod, E., Chmura, G.L., Bouillon, S., Salm, R., Björk, M., Duarte, C.M., Lovelock, C.E., Schlesinger, W.H., Silliman, B.R., 2011. A blueprint for blue carbon: toward an improved understanding of the role of vegetated coastal habitats in sequestering CO_2. Front. Ecol. Environ. 9, 552–560.

Mejía-Piña, K.G., Huerta-Diaz, M.A., González-Yajimovich, O., 2016. Calibration of handheld X-ray fluorescence (XRF) equipment for optimum determination of elemental concentrations in sediment samples. Talanta 161, 359–367.

Moreno, A., Belmonte, A., Bartolomé, M., Sancho, C., Oliva, B., Stoll, H., Edwards, L.R., Cheng, H., Hellstrom, J., 2013. Formación de espeleotemas en el Noreste Peninsular y su relación con las condiciones climáticas durante los últimos ciclos glaciares. Cuad. Investig. Geogr. 39, 25–47.

Morford, J.L., Emerson, S., 1999. The geochemistry of redox sensitive trace metals in sediments. Geochim. Cosmochim. Acta 63, 1735–1750.

Morse, J.W., 2003. Formation and diagenesis of carbonate sediments. In: Mackenzie, F.T. (Ed.), Sediments, Diagenesis, and Sedimentary Rocks. vol. 7. Elsevier-Pergamon, Oxford, pp. 67–85.

Morse, J.W., Arvidson, R.S., 2002. The dissolution kinetics of major sedimentary carbonate minerals. Earth-Sci. Rev. 58, 51–84.
Morse, J.W., Mackenzie, F.T., 1990. Geochemistry of Sedimentary Carbonates. Elsevier, Amsterdam 709 p.
Mount, J.F., 1984. Mixing of siliciclastic and carbonate sediments in shallow shelf environments. Geology 12, 432–435.
Opdyke, B.D., Walker, J.C.G., 1992. Return of the coral reef hypothesis: basin to shelf partitioning of $CaCO_3$ and its effects on atmospheric CO_2. Geology 20, 733–736.
Orcutt, B.N., Joye, S.B., Kleindienst, S., Knittel, K., Ramette, A., Reitz, A., Samarkin, V., Treude, T., Boetius, A., 2010. Impact of natural oil and higher hydrocarbons on microbial diversity, distribution, and activity in Gulf of Mexico. Deep-Sea Res. II 57, 2008–2021.
Parsons, C., Grabulosa, E.M., Pili, E., Floor, G.H., Roman-Ross, G., Charlet, L., 2013. Quantification of trace arsenic in soils by field-portable X-ray fluorescence spectrometry: Considerations for sample preparation and measurement conditions. J. Hazard. Mater. 262, 1213–1222.
Potts, P.J., Williams-Thorpe, O., Webb, P.C., 1997. The bulk analysis of silicate rocks by portable X-ray fluorescence: effect of sample mineralogy in relation to the size of the excited volume. Geostand. Newslett. 21, 29–41.
Potts, P.J., Bernardini, F., Jones, M.C., Williams-Thorpe, O., Webb, P.C., 2006. Effects of weathering on *in situ* portable X-ray fluorescence analyses of geological outcrops: dolerite and rhyolite outcrops from the Preseli Mountains, South Wales. X-Ray Spectrom. 35, 8–18.
Quye-Sawyer, J., Vandeginste, V., Johnston, K.J., 2015. Application of handheld energy-dispersive X-ray fluorescence spectrometry to carbonate studies: opportunities and challenges. J. Anal. At. Spectrom. 30, 1490–1499.
Rabouille, C., Caprais, J.-C., Lansard, B., Crassous, P., Dedieu, K., Reyss, J.L., Khripounoff, A., 2009. Organic matter budget in the Southeast Atlantic continental margin close to the Congo Canyon: in situ measurements of sediment oxygen consumption. Deep-Sea Res. II 56, 2223–2238.
Reinhard, C.T., Planavsky, N.J., Wang, X., Fischer, W.W., Johnson, T.M., Lyons, T.W., 2014. The isotopic composition of authigenic chromium in anoxic marine sediments: a case study from the Cariaco Basin. Earth Planet. Sci. Lett. 407, 9–18.
Ridgwell, A., Zeebe, R.E., 2005. The role of the global carbonate cycle in the regulation and evolution of the Earth system. Earth Planet. Sci. Lett. 234, 299–315.
Roberts, H.H., 1987. Modern carbonate-siliciclastic transitions: humid and arid tropical examples. Sediment. Geol. 50, 25–65.
Roberts, H.H., Murray, S.P., 1988. Gulfs of the Northern Red Sea: depositional settings of abrupt siliciclastic-carbonate transitions. In: Doyle, L.J., Roberts, H.H. (Eds.), Carbonate-Clastic Transitions. Elsevier, Amsterdam, pp. 99–142.
Roberts, A.P., Florindo, F., Chang, L., Heslop, D., Jovane, L., Larrasoaña, J.C., 2013. Magnetic properties of pelagic marine carbonates. Earth-Sci. Rev. 127, 111–139.
Rodríguez-Navarro, A., Jimenez-Lopez, C., Hernandez-Hernandez, A., Checa, A., García-Ruiz, J.M., 2008. Nanocrystalline structures in calcium carbonate biominerals. J. Nanophotonics 2, 021935. https://doi.org/10.1117/1.3062826.
Rowe, H., Hughes, N., Robinson, K., 2012. The quantification and application of handheld energy-dispersive x-ray fluorescence (ED-XRF) in mudrock chemostratigraphy and geochemistry. Chem. Geol. 324/325, 122–131.
Runge, E.J., 1966. Continental Shelf Sediments, Columbia River to Cape Blanco. Oregon State University, Oregon Ph.D. Dissertation. 143 p.
Ryba, S.A., Burgess, R.M., 2002. Effects of sample preparation on the measurement of organic carbon, hydrogen, nitrogen, sulfur, and oxygen concentrations in marine sediments. Chemosphere 48, 139–147.
Saderne, V., Geraldi, N.R., Macreadie, P.I., Maher, D.T., Middelburg, J.J., Serrano, O., Almahasheer, H., Arias-Ortiz, A., Cusack, M., Eyre, B.D., Fourqurean, J.W., Kennedy, H., Krause-Jensen, D., Kuwae, T., Lavery, P.S., Lovelock, C.E., Marba, N., Masqué, P., Mateo, M.A., Mazarrasa, I., McGlathery, K.J., Oreska, M.P.J., Sanders, C.J., Santos, I.R., Smoak, J. M., Tanaya, T., Watanabe, K., Duarte, C.M., 2019. Role of carbonate burial in blue carbon budgets. Nat. Commun. 10, 1106. https://doi.org/10.1038/s41467-019-08842-6.
Saker-Clark, M., Kemp, D.B., Coe, A.L., 2019. Portable X-ray fluorescence spectroscopy as a tool for cyclostratigraphy. Geochem. Geophys. Geosyst. 20, 2531–2541.
Sanders, C.J., Maher, D.T., Smoak, J.M., Eyre, B.D., 2019. Large variability in organic carbon and $CaCO_3$ burial in seagrass meadows: a case study from three Australian estuaries. Mar. Ecol. Prog. Ser. 616, 211–218.
Santisteban, J.I., Mediavilla, R., López-Pamo, E., Dabrio, C.J., Ruiz Zapata, M.B., Gil García, M. J., Castaño, S., Martínez-Alfaro, P.E., 2004. Loss on ignition: a qualitative or quantitative method for organic matter and carbonate mineral content in sediments? J. Paleolimnol. 25, 287–299.
Schneider, R.R., Schulz, H.D., Hensen, C., 2000. Marine carbonates: their formation and destruction. In: Schulz, H.D., Zabel, M. (Eds.), Marine Geochemistry. Springer, Berlin, pp. 283–308.
Schroeder, J.O., Murray, R.W., Leinen, M., Pflaum, R.C., Janecek, T.R., 1997. Barium in equatorial Pacific carbonate sediment: terrigenous, oxide, and biogenic associations. Paleoceanography 12, 125–146.
Schropp, S.J., Lewis, F.G., Windom, H.L., Ryan, J.D., 1990. Interpretation of metal concentrations in estuarine sediments of Florida using aluminum as a reference element. Estuaries 13, 227–235.
Sinnesael, M., de Winter, N.J., Snoeck, C., Montanari, A., Claeys, P., 2018. An integrated pelagic carbonate multi-proxy study using portable X-ray fluorescence (pXRF): Maastrichtian strata from the Bottaccione Gorge, Gubbio, Italy. Cretac. Res. 91, 20–32.
Tatzber, M., Stemmer, M., Spiegel, H., Katzlberger, C., Haberhauer, G., Gerzabek, M.H., 2007. An alternative method to measure carbonate in soils by FI-IR spectroscopy. Environ. Chem. Lett. 5, 9–12.
Tjallingii, R., Röhl, U., Kölling, M., Bickert, T., 2007. Influence of the water content on X-ray fluorescence core-scanning measurements in soft marine sediments. Geochem. Geophys. Geosyst. 8, Q02004. https://doi.org/10.1029/2006GC001393.
Tribovillard, N., du Châtelet, E.A., Gay, A., Barbecot, F., Sansjofre, P., Potdevin, J.-L., 2013. Geochemistry of cold seepage-impacted sediments: Per-ascensum or per-descensum trace metal enrichment? Chem. Geol. 340, 1–12.
Turekian, K.K., Wedepohl, K.H., 1961. Distribution of the elements in some major units of the Earth's crust. Geol. Soc. Am. Bull. 72, 175–192.
Vanhoof, C., Corthouts, V., Tirez, K., 2004. Energy-dispersive X-ray fluorescence systems as analytical tool for assessment of contaminated soils. J. Environ. Monit. 6, 344–350.
Wallmann, K., Aloisi, G., Haeckel, M., Tishchenko, P., Pavlova, G., Greinert, J., Kutterolf, S., Eisenhauer, A., 2008. Silicate weathering in anoxic marine sediments. Geochim. Cosmochim. Acta 72, 2895–2918.
Wang, J., Zhu, L., Wang, Y., Gao, S., Daut, G., 2012a. A comparison of different methods for determining the organic and inorganic carbon content of lake sediment from two lakes on the Tibetan Plateau. Quat. Int. 250, 49–54.
Wang, X., Wang, J., Zhang, J., 2012b. Comparisons of three methods for organic and inorganic carbon in calcareous soils of Northwestern China. PLoS One 7, e44334. https://doi.org/10.1371/journal.pone.0044334.
Ward, C.H., Tunnell Jr ., J.W., 2017. Chapter 1. Habitats and biota of the Gulf of Mexico: an overview. In: Ward, C.H. (Ed.), Habitats and Biota of the Gulf of Mexico: Before the Deepwater Horizon Oil Spill. Volume 1: Water Quality, Sediments, Sediment Contaminants, Oil and Gas Seeps, Coastal Habitats, Offshore Plankton and Benthos, and Shellfish. Springer Open, New York, pp. 1–54.
Ward, W.C., Wilson, J.L., 1976. General aspects of the northeastern coast of the Yucatan Peninsula. In: Weidie, A.E., Ward, W.C. (Eds.), Carbonate Rocks and Hydrogeology of the Yucatan Peninsulam Mexico. Geological Society of America, New Orleans, pp. 35–44.
Wei, G., Liu, Y., Li, X., Chen, M., Wei, W., 2003. High-resolution elemental records from the South China Sea and their paleoproductivity implications. Paleoceanogr. Paleocl. 18, 1–12.
Yuan, Z., Cheng, Q., Xia, Q., Yao, L., Chen, Z., Zuo, R., Xu, D., 2014. Spatial patterns of geochemical elements measured on rock surfaces by portable X-ray fluorescence: application to hand specimens and rock outcrops. Geochem. Explor. Environ. Anal. 14, 265–276.
Zhang, S., Wang, X., Wang, H., Bjerrum, C.J., Hammarlund, E.U., Costa, M.M., Connelly, J.N., Zhang, B., Su, J., Canfield, D.E., 2016. Sufficient oxygen for animal respiration 1400 million years ago. Proc. Natl. Acad. Sci. 113, 1731–1736.